forests

MDPI

Article

Urban Forest Microclimates and Their Response to Heat Waves—A Case Study for London

David Hidalgo-García [1], Dimitra Founda [2], Hamed Rezapouraghdam [3,4,*], Antonio Espínola Jiménez [1] and Muaz Azinuddin [4]

[1] Technical Superior School of Building Engineering, Universidad de Granada, 18071 Granada, Spain; dhidalgo@ugr.es (D.H.-G.); antonioespinola@ugr.es (A.E.J.)
[2] Institute for Environmental Research and Sustainable Development, National Observatory of Athens, P. Penteli, GR-15236 Athens, Greece; founda@noa.gr
[3] Faculty of Tourism, Eastern Mediterranean University, TRNC, Via Mersin 10, Gazimagusa 99628, Turkey
[4] Faculty of Applied Social Science, University Sultan Zainal Abidin, Gong Badak Campus, Terengganu 21300, Malaysia; muazazinuddin@unisza.edu.my
* Correspondence: hamed.rezapouraghdam@emu.edu.tr

Abstract: Extreme weather events and rising temperatures pose significant risks, not only in urban areas but also in metropolitan forests, that affect the well-being of the people who visit them. City forests are considered one of the best bets for mitigating high temperatures within civic areas. Such areas modulate microclimates in contemporary cities, offering environmental, social, and economic advantages. Therefore, comprehending the intricate relationships between municipal forests and the climatic changes of various destinations is crucial for attaining healthier and more sustainable city environments for people. In this research, the thermal comfort index (Modified Temperature–Humidity Index (MTHI)) has been analysed using Landsat images of six urban forests in London during July 2022, when the area first experienced record-breaking temperatures of over 40 °C. Our results show a significant growth in the MTHI that goes from 2.5 (slightly hot) under normal conditions to 3.4 (hot) during the heat wave period. This situation intensifies the environmental discomfort for visitors and highlights the necessity to enhance their adaptability to future temperature increases. In turn, it was found that the places most affected by heat waves are those that have grass cover or that have small associated buildings. Conversely, forested regions or those with lakes and/or ponds exhibit lower temperatures, which results in enhanced resilience. These findings are noteworthy in their concentration on one of the UK's most severe heat waves and illustrate the efficacy of integrating spectral measurements with statistical analyses to formulate customized regional initiatives. Therefore, the results reported will allow the implementation of new planning and adaptation policies such as incorporating thermal comfort into planning processes, improving green and blue amenities, increasing tree densities that are resilient to rising temperatures, and increasing environmental comfort conditions in metropolitan forests. Finally, the applicability of this approach in similar urban contexts is highlighted.

Keywords: microclimate; urban forests; vegetation; heat waves; heat mitigation; remote sensing

Academic Editor: Lei Wang

Received: 2 April 2025
Revised: 2 May 2025
Accepted: 7 May 2025
Published: 8 May 2025

Citation: Hidalgo-García, D.; Founda, D.; Rezapouraghdam, H.; Jiménez, A.E.; Azinuddin, M. Urban Forest Microclimates and Their Response to Heat Waves—A Case Study for London. *Forests* **2025**, *16*, 790. https://doi.org/10.3390/f16050790

1. Introduction

In recent decades, there has been an increase in extreme weather events such as floods, droughts, and cold and heat waves related to the global warming process that is taking

place on the planet. It is possible to classify this issue as one of the greatest challenges for human beings [1–4]. At the same time, the modification and transformation of the different surface covers for the construction of new urban areas motivated by significant population growth is one of the processes that contribute most to global warming [1,5,6]. Urban areas reduce evapotranspiration [7] because they are built with impermeable materials, such as asphalt and concrete. These have high thermal absorption and store the heat received from solar radiation, which is subsequently released into the atmosphere [8,9]. In addition to this circumstance, the United Nations (UN) predicted in a 2020 report that by 2050, 70% of the population will be in these areas [10], which will mean significant growth in these areas [11]. Numerous studies report that urban areas suffer the greatest increases in temperatures [12–14], mainly affected by anthropogenic heat, environmental pollution, and the phenomenon of urban heat islands (UHIs) [15]. Currently, 30% of the world's population suffers from extreme heat conditions, and the forecast is that by 2050, it will reach 74% [16].

Recent studies have shown that heat waves are more intense, longer, and more frequent [17–19]. These same studies estimate that they will affect larger land areas [9,20] by the end of the twenty-first century. These episodes of rising temperatures are identified as one of the natural phenomena with the greatest impact on the population [19] that will affect people's quality of life, especially in residents of urban areas. To counteract this increase in temperatures in urban areas, several studies consider that the homogeneous distribution of trees in the streets, the use of Urban Green Infrastructures (UGIs), and the use of open and unpaved spaces are some of the most effective strategies. These proposals make it possible to mitigate urban heat and improve human comfort [21–24]. Green areas located within cities minimize temperatures and reduce the intensity of the UHI phenomenon. In this way, inhabitants can enjoy these more comfortable areas that tend to be cooler during hot periods, which improves the quality of life. The shadows generated by trees in green areas prevent impermeable surfaces from being heated by solar radiation [6]. In turn, the evapotranspiration of plant elements increases ambient humidity and minimizes temperatures, producing widespread ambient cooling [22–24].

The term Park Cool Island (PCI) is used to describe the temperature differences between urban areas and green spaces [25]. This phenomenon has been routinely studied in recent years in many cities worldwide, where decreased temperatures are recorded at green parks compared to urban built areas. For instance, according to a 2018 study focused on the city of Mumbai (India), green areas recorded average temperatures between 2 and 3 °C lower than urbanized areas [26]; another study carried out between 2005 and 2015 in the city of Singapore reported a temperature difference of between 1 and 3 °C in green areas [27]; additionally, the study carried out in the city of Shenzhen (China) denoted differences of 1.0 and 1.6 °C between 2011 and 2013 [28]. Moreover, research carried out in four green areas of the city of Wroclaw (Poland) showed a reduction in temperatures of between 1 and 2 °C. Conversely, the studies conducted at Osaka Prefecture Campus University [29] and in the cities of Vancouver and Sacramento (USA) are noteworthy, indicating that tree-covered green areas most effectively lower daytime temperatures, whereas grass-covered areas are more effective at night [30]. Therefore, it seems proven that green areas allow for temperatures of urban areas to be minimized and the effects of high temperatures to be mitigated, being considered comfort zones for the population. However, although there are some studies examining the mitigating effect of temperatures and the consequent impact on human thermal comfort during heat waves, these are scarce in the area under study. This is possibly due to the scarcity of heat waves that the United Kingdom has experienced. Thus, according to data from the Meteorological Office (Met Office), only 15 heat waves have occurred since 1808. However, 50% occurred in the 21st

century, with a significant upward trend being observed [31]. This study aims to address this deficiency by evaluating, for the first time in the United Kingdom, the effects of a heat wave on thermal comfort in green spaces using the MTHI.

Several indicators or indices have been proposed to assess thermal comfort conditions in urban areas, including the Comfort Index (CI), the Thermal Climate Comfort Index (UTCI), and the MTHI. The latter, when obtained through satellite images, has the advantage of having a higher spatial resolution than the rest by maintaining the pixel size of the images. On the other hand, the data are more easily accessible than those needed to determine other indices. There are many studies in the literature that have used this index to determine thermal comfort in urban areas. For instance, the study carried out in Shanghai (China) in 2024 using Landsat imagery reported that this methodology is adequate to obtain thermal comfort due to the excellent results [32], and the study carried out in the city of Jiangsu (China) in 2020 with Landsat 5 and 8 imagery reported that the MTHI based on remote sensing can monitor the spatial distribution of thermal comfort, being an adequate index for these studies [33].

Despite advances in the study of the effect of green areas on urban temperature mitigation, significant gaps remain in our understanding of how this process evolves during extreme heat events, such as heat waves. Understanding this evolution is crucial for the effective implementation of design strategies in the planning and construction of new green areas. While previous research has explored this relationship, it has done so primarily through in situ measurements, without considering a comprehensive and dynamic view of the phenomenon, but also aspects related to human thermal comfort. This research introduces a novel approach by analyzing the thermal resilience of green areas from a multifactorial perspective, considering the characteristics of plant systems and construction and design aspects. Through the use of high-precision satellite images, combined with remote sensing techniques and thermal comfort analysis, this study offers an innovative insight into the microclimate generated in these green areas unaccustomed to extreme temperatures. This contribution is key not only to the planning of green spaces in the city of London but also to the development of strategies applicable to other regions of the world.

Based on what was discussed above, this research aims to analyse thermal comfort using the MTHI at six green areas in the city of London, to determine their resilience in extreme heat conditions. Over the course of summer 2022, the UK was hit by a sequence of heat waves, resulting in approximately 3000 excess deaths [31,34,35]. The date 19 July 2022 has been assigned as a historic day for the UK's climate, signifying a milestone in the country's environmental temperature records. Five weather stations from London to Lincolnshire reached 40 °C or more, breaking previous all-time records. A national emergency was declared by the government in July 2022, following the first ever 'red' extreme heat warning and the first Level 4 heat wave alert issued by the UK Health Security Agency and Met Office [31,34,35]. In this sense, the specific geographical location of this research, combined with the exceptional climate situation affecting the United Kingdom during the study period, gives this work a remarkable originality. The uniqueness of the conditions analyzed not only offers a unique opportunity to advance knowledge in this field but also provides empirical evidence that is difficult to replicate in other geographical and climatic contexts. These exceptional circumstances, therefore, reinforce the innovative contribution of this research to the international academic debate.

For the development of this work, and based on Landsat images, the different Land Use/Land Cover (LULC) categories were determined in order to delimit the green areas of the city. Next, and for each green area and environmental condition, the Normalized Difference Vegetation Index (NDVI), the Normalized Difference Moisture Index (NDMI), and Land Surface Temperature (LST) were obtained. To identify correlations between variables,

statistical techniques such as Panel Data and ANOVA were applied. The questions raised in this study are: 1. How are LST, NDMI, and NDVI values developed in the green spaces studied using Landsat imagery? 2. What thermal comfort conditions do the green areas experience under normal summer conditions, and what variability do they show when the heat intensifies due to the heat wave phenomenon? 3. Is there any relationship between the indices considered that would improve the thermal comfort of green areas? 4. Could the findings be useful for future green area development, given that heat waves are expected to become more frequent and intense in the coming years?

In addition, our research addresses the need for prompt action to be taken by the United Nations to reduce the effects of climate change and its repercussions all over the world by providing new urban planning and adaptation strategies that are resistant to increasing temperatures and that boost environmental comfort conditions in urban forests.

This research contributes to the understanding of the effect that heat waves will have on the thermal comfort of people in green areas of the city of London. A foreseeable deterioration in the thermal comfort of these areas during high temperatures would demonstrate their vulnerability to the effects of climate change, emphasizing the need to develop new mitigation and adaptation strategies for these spaces so that they can continue to offer thermal comfort benefits to the inhabitants. Furthermore, this methodological approach that combines satellite data allows for a robust and generalized perspective for the study of other green areas located in other cities. Finally, the research establishes an empirical basis that underlines the need to integrate thermal comfort into the planning and management of urban green spaces within the context of climate change. This will encourage urban planners and public administrations to plan more appropriately for the creation of green areas and spaces capable of adapting to climate change, thereby promoting the well-being of the population.

2. Materials and Methods

2.1. Study Area

The areas under study are located within the city of London (United Kingdom) (Figure 1). The UTM geographical coordinates of the city are latitude 51°30′26″ N and longitude 0°07′39″ W. It is located at an altitude of 24 m above sea level. The city has a population of 8.86 million and covers an area of 1572 km^2. The city's climate is of the mid-latitude oceanic type (Cfb), according to Koppen–Geiger, which implies warm summers and cool winters with abundant rainfall. The average temperature and number of hours of sunshine per year are 13.8 °C and 1496, respectively. This gives an average of 4.10 h of sunshine per day.

Six urban forests in London were selected, varying in soil type and size and located within the city boundaries. The criteria for selecting the green areas were as follows: large surface area (>45 hectares), location in the city center so that it could not be affected by the surrounding urban areas and that they would have a high influx of visitors. Their location is shown in Figure 2, while their area, dimensions, cover, and morphology are detailed in Table 1 and Figure S1 in the Supplementary Materials.

2.2. Methodology

The methodology carried out for this research is described in Figure 3. To start, it was necessary to download the Landsat 8 and 9 images. The month of July 2022 has been chosen as it was extremely hot, with the 19th being the first time in the history of the city that the value of 40 °C was recorded. The images were obtained from the United States Geological Survey (USGS) and underwent an atmospheric correction process. Next, a plan of bands 2, 3, and 4 (RGB) was composed to obtain the different LULCs of the city using the

Random Forest (RF) methodology to categorize the covers (Water, Vegetation, Urban land, and Farmland). Precision was determined using a precision matrix [36,37]. Next, and for each selected green area, the NDVI and NDMI related to vegetation and soil moisture were obtained. The LST was obtained from thermal band number 10 of the Landsat. With these variables, the MTHI could be determined under usual summer environmental conditions and under heat wave conditions. The relationships between the variables LST, NDMI, and MTHI can be visualized in Figure S2 of the Supplementary Materials. Both the LST and the NDMI variables required to obtain the MTHI were validated using data from the Met Office-approved meteorological station located in London Marylebone Road. To carry out the statistical analysis, version 16 of the STATA data science software was used. It combined the data panel with ANOVA tests to evaluate significant variations in MTHI values between zones and periods.

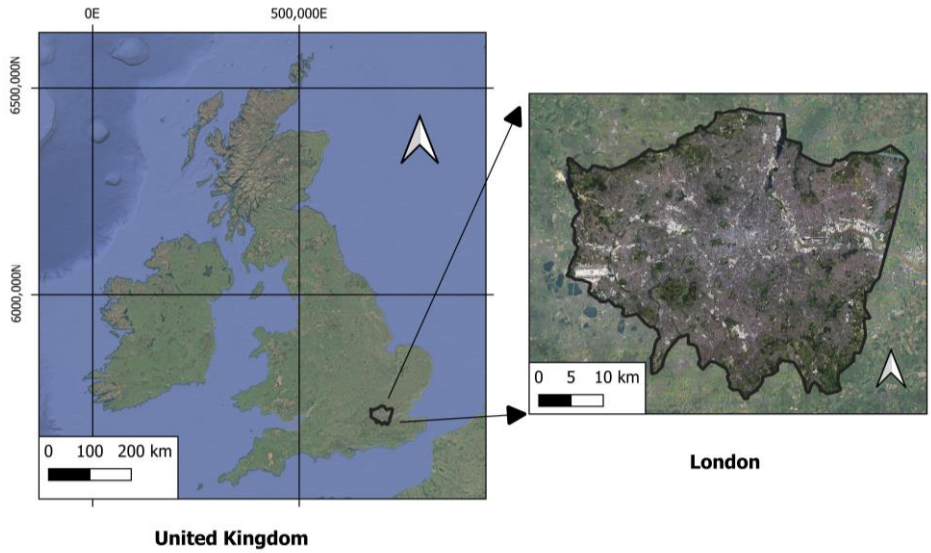

Figure 1. Study area: London, United Kingdom.

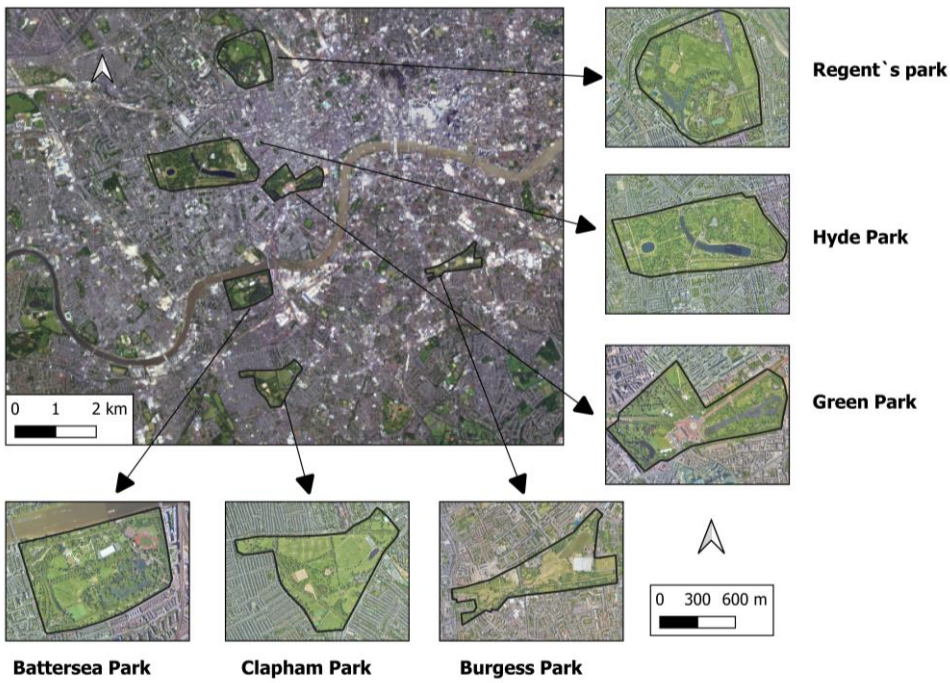

Figure 2. The 6 green areas of London selected for the study.

Table 1. Characteristics of the green areas selected for the study, based on the selection criteria.

Area	Name	Surface Area (Ha)	Perimeter (m)	LSI	Aquatic Area (Ha)	Soil Type	Ground Cover
1	Regent's Park	138.69	4407	1.055	5.04	Vegetation	1
2	Hyde Park	250.91	5759	1.207	10.80	Vegetation	1
3	Green Park	72.74	4231	1.401	7.02	Vegetation	1
4	Battersea Park	80.67	3602	1.131	5.40	Vegetation	1
5	Clapham Park	81.91	4443	0.985	1.80	Vegetation	1
6	Burgess Park	45.40	4346	1.382	3.50	Vegetation	1

Note: LSI: Landscape Shape Index. (1): Trees, lawn, and lake.

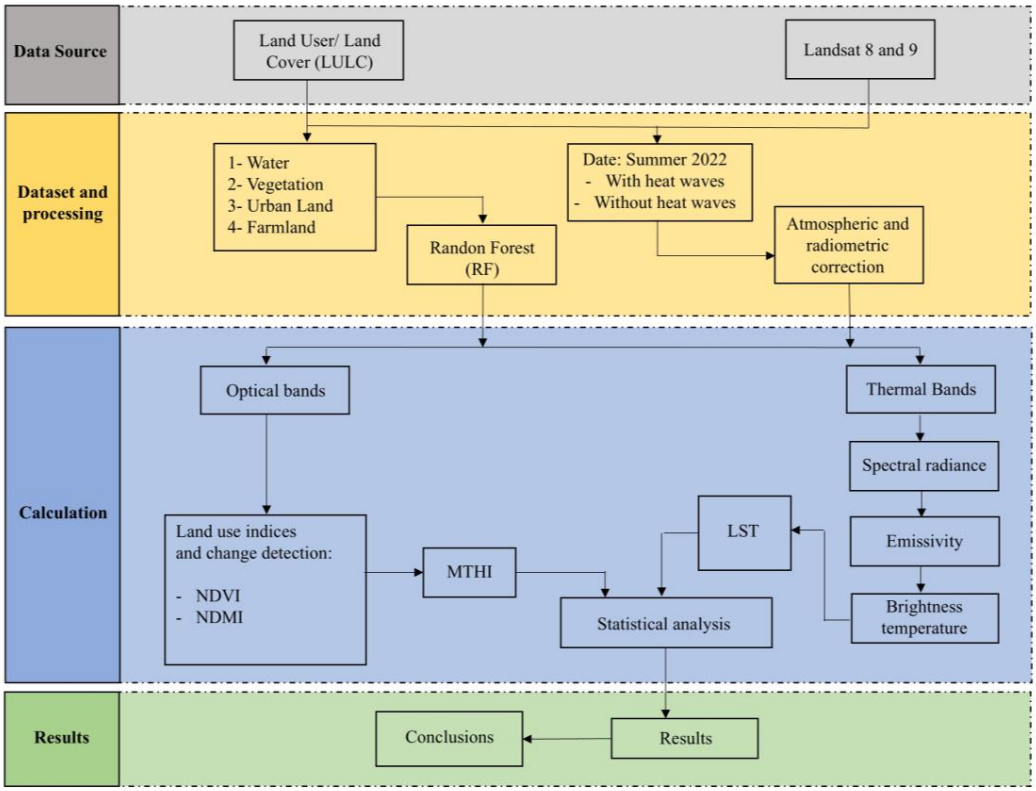

Figure 3. Research framework and methodological approach.

2.3. Landsat Images

Table 2 details the Landsat 8 and 9 imageries used in this study. The satellites are equipped with 8 multispectral bands (bands 1 to 7 and 9) with a resolution of 30 m, in addition to two thermal infrared bands (bands 10 and 11) that have a spatial resolution of 100 m. However, for the calculation of the LST, the thermal bands were resampled at a resolution of 30 m, and only band 10 was used for the calculation. Atmospheric correction of the bands was performed by applying the Dark Object Subtraction (DOS) algorithm [38,39] using the semi-automatic classification plugin (SCP) in QGIS, a free software [40].

Table 2. Landsat images used in the research.

Products	Environmental Condition	Date (yyyymmdd)	UTC Time (hhmm)	Cloud Cover (%)
LC08_L1TP_201024_20220710_T1	No Heat Wave	20220710	10:50	4.76
LC09_L2SP_201024_20220718_T1	Heat Wave	20220718	10:48	0.38

Since the UK experienced a series of heat waves during the summer of 2022, resulting in the deaths of a significant number of people, and since 19 July of that year was the day temperatures exceeded 40 °C for the first time in history, a Landsat dataset from July

2022 with low cloud cover (<5%) was selected. Low cloud cover images allow for better discrimination of different land uses and typologies. For July 2022, Landsat only has three images: 10, 18, and 26 July. Under these conditions, two images were obtained: one representative of normal environmental conditions (10 July, (26 July had a cloud cover index above 5%)), and another (July 18) for the heat wave.

2.4. Spectral Indices and LST Landsat

Table 3 shows the equations used to determine the indices and LST.

Table 3. Landsat indices.

Index	Equation	Number	Reference
NDVI	$\frac{NIR-Red}{NIR+Red}$	(1)	[41]
NDMI	$\frac{NIR-SWIR}{NIR+SWIR}$	(2)	[42]
Spectral Radiance	$L_\lambda = M_L \times Q_{Cal} + A_L$	(3)	[43]
Brightness Temperature (°C)	$T = \frac{K_2}{log\left(\frac{K_1}{L_\lambda}+1\right)} - 273.15$	(4)	[44]
Land Surface Emissivity	$\varepsilon = 0.004 \times Pv + 0.986$	(5)	[44,45]
PV	$PV = \left(\frac{NDVI-NDVI_{Min}}{NDVI_{Max}-NDVI_{Min}}\right)^2$	(6)	[44]
LST (°C)	$LST = \frac{T}{\left(1+\left(\lambda \frac{T}{C_2}\right)\times log(\varepsilon)\right)}$	(7)	[44]

Note: NIR, RED, and SWIR: Bands 5, 4, and 6 Landsat 8 and 9. M_L: is the specific multiplying factor located in the metadata index Landsat. Q_{cal}: is the digital variant value. A_L: is the additive factor of specific re-scaling of TIRS bands. K_1 = 774.8553. K_2 = 1321.0789. C_2 = 1.4388 *10^{-2} m*K. λ = 10.8 µm.

2.5. LULC

Using bands 2, 3, and 4 of the Landsat satellites, a true-color (RGB) image was composed. Subsequently, using the QGIS software and the RF method, the LULC classification image was obtained. This technique has been widely used in studies on the classification of different land covers [13,46,47] due to its high accuracy [48]. In this study and for the city of London, four main land covers of soil have been identified: vegetation, water, urban land, and farmland.

2.6. LSI

This variable measures the relationship between the perimeter of a green area and its surface area. If the result reports a value close to 1, it indicates that the area's shape approximates a circle. If, on the other hand, the values are greater than 1, it indicates that the area has polygonal or irregular shapes. This variable is frequently used in research related to green areas [21,49]. It is calculated using Equation (8):

$$LSI = \frac{L}{2 \times \sqrt{A \times \pi}} \quad (8)$$

where L represents the total length of the perimeter of the studied area and A is the corresponding area.

2.7. MTHI

Urban thermal comfort was used to determine the degree of perception of people of the environmental thermal conditions of the selected green spaces. As it is obtained using satellite images, it has the advantages of having a high resolution and the data necessary to obtain it (NDMI and LST) are easily accessible. The MTHI is obtained by Equation (9) [32]:

$$\text{MTHI} = 1.8 \times \text{LST} + 32 - 0.55 \times (1 - \text{NDMI}) \times (1.8 \times \text{LST} - 26) \quad (9)$$

where the LST is obtained from Equations (3)–(7) and the NDMI from Equation (2). The MTHI obtained presents dimensionless numerical values that are subsequently reclassified into five categories established by the authors [32] and according to Table 4. To do this, it has been necessary to obtain the mean values and the standard deviation of the MTHI values that are within the limit of each green zone investigated for each satellite image and, therefore, for each environmental condition.

Table 4. Classification of outdoor thermal comfort levels [32].

MTHI	Equation	Type
1	$MTHI < M - 1.5 \times a$	Cool
2	$M - 1.5 \times a \leq MTHI < M - 0.5 \times a$	Slightly hot
3	$M - 0.5 \times a \leq MTHI < M + 0.5 \times a$	Hot
4	$M + 0.5 \times a \leq MTHI < M + 1.5 \times a$	Very hot
5	$M + 1.5 \times a \leq MTHI$	Extremely hot

Note: M: mean MTHI value; a: MTHI standard deviation.

2.8. Statistical Methodology

Due to the presence of data from various indices and variables across multiple green spaces in the city, along with time series data spanning several days in July, it was essential to employ two methodological approaches: Analysis of Variance (ANOVA) and data panel. The first statistical approach allowed us to identify that there are statistically significant differences in the variables analyzed in the different green areas by comparing variances. Data panel is the methodology that allows combining time values with data or other values of a transversal nature. This method is commonly cited in the literature and uses multiple regression models [50–52], which makes it possible to incorporate a larger amount of data compared to traditional methods.

3. Results

3.1. LULC

The spatiotemporal analysis of the different LULC categories and their occupancy percentage in the city of London can be seen in Figure 4. As can be seen, the city of London had predominantly urban land (74.65%) followed by vegetation (15.76%), farmland (6.19%), and water (3.40%). The results of the precision matrix carried out using Landsat 8 images to check the LULC plane were as follows: the overall accuracy obtained by the precision matrix was 91% with a 95% confidence interval ranging from 0.80 to 0.91 points. However, and for the investigation carried out, a subsequent manual correction of the non-coinciding points was carried out.

3.2. Spatiotemporal Evaluation of NDVI and NDMI

The spatiotemporal analysis of the NDVI and NDMI in the studied areas under normal environmental conditions and heat waves can be seen in Figures S3–S6 in the Supplementary Materials. Figures 5 and 6 illustrate the index values for various LULC classes for the entire city (a) and for each of the green areas investigated (b). All this under the two different environmental conditions investigated. The NDVI enables the distinction between vegetated areas and artificial land without vegetation. This provides information on the health status of the vegetation located on the Earth's surface. On the other hand, the NDMI helps assess the moisture content present in both vegetation and soil. High NDVI and NDMI values indicate high humidity and healthy vegetation. Conversely, low values indicate plant stress due to moisture loss in both vegetation and soil.

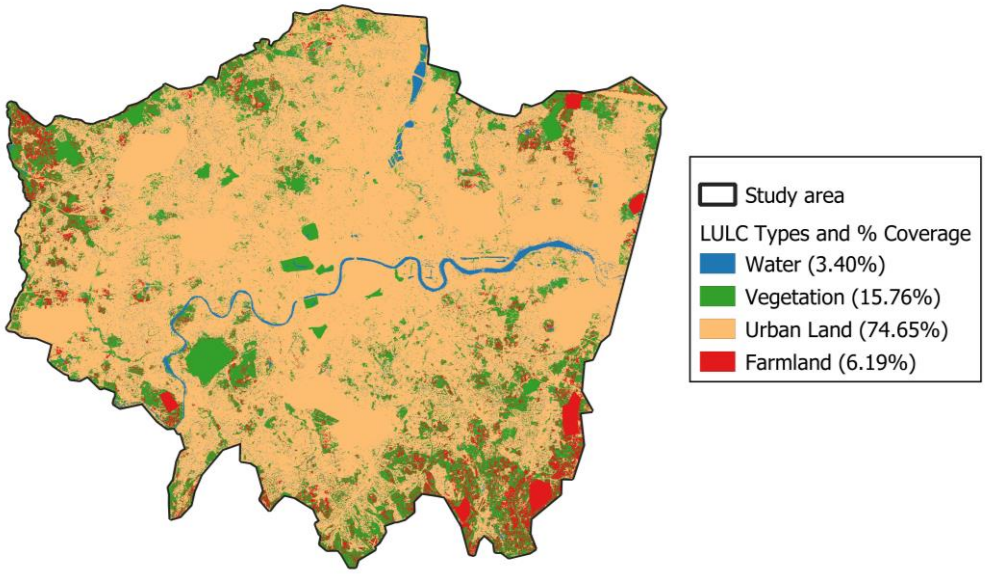

Figure 4. LULC coverage of the city of London using Random Forest methodology.

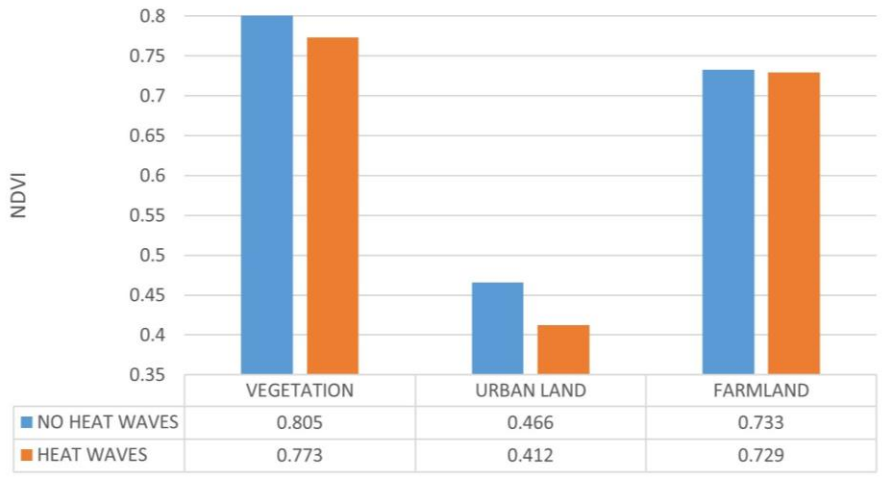

(a)

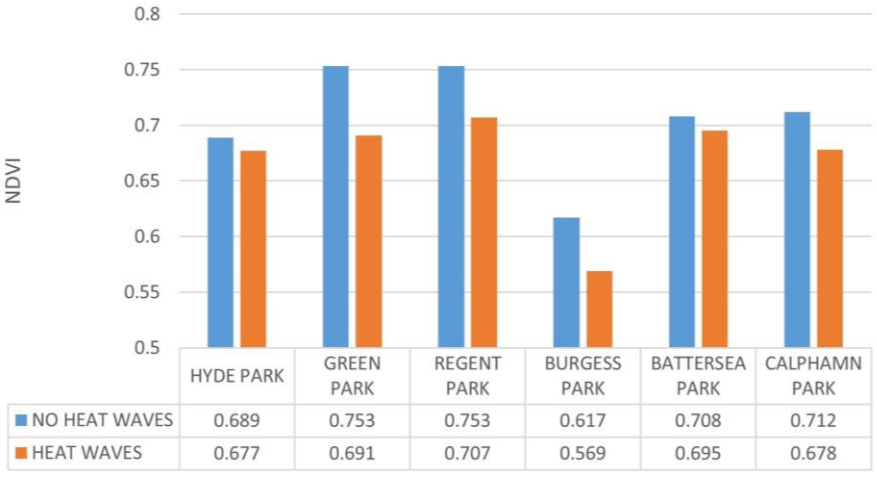

(b)

Figure 5. NDVI under heat wave and non-heat wave (normal) environmental conditions by different LULC classes of the city (**a**) and by different green areas (**b**).

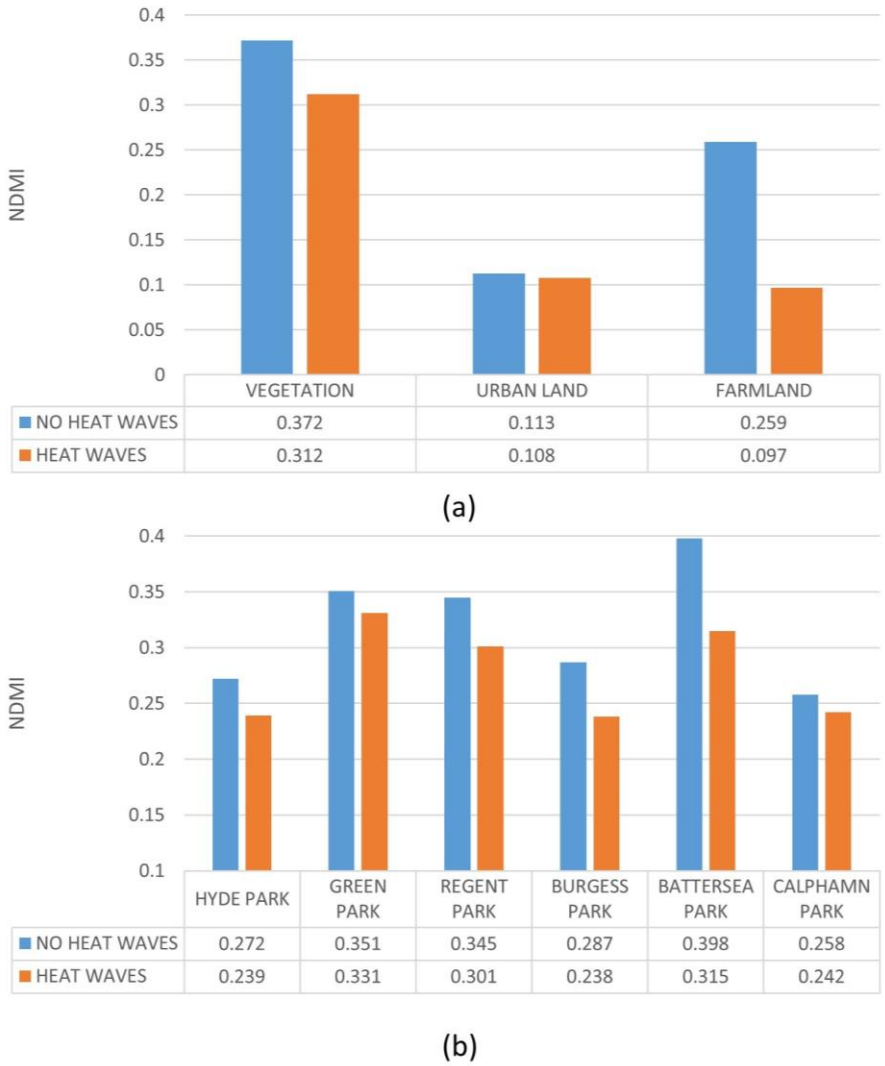

Figure 6. NDMI under heat wave and non-heat wave (normal) environmental conditions by different LULC classes of the city (**a**) and by different green areas (**b**).

The NDVI presents higher values under normal conditions than under heat wave conditions in the different LULC categories (Figure 5a). Thus, under normal conditions, the highest average value (0.805) is in the vegetation cover, while the lowest value (0.466) is in the urban land cover. Farmland coverage has a value of 0.733. Under heat wave conditions, the variation in the NDVI between the different LULC classes follows the same pattern but with a generalized decrease of 3.97%, 11.58%, and 0.54% in vegetation, urban land, and farmland coverage, respectively. Concerning each of the green areas analysed and under normal environmental conditions, the average value of the NDVI is 0.705, ranging from the highest (0.753) for Regent's Park and Green Park to the lowest (0.617) for Burgess Park (Figure 5b). This is because the former have larger areas of vegetation and tree cover, allowing for higher NDVI values. The values suffer a generalized decrease under heat wave conditions, so that the average value is 0.669. This represents an average decrease of 5.04%, which translates into a deterioration in plant health. The largest declines were reported in Green Park (−8.23%), Burgess Park (−7.78%), and Regent's Park (−6.11%). These, and due to the greater tree mass and the rise in temperatures, suffer the effects of heat to a greater extent through a significant decrease in the NDVI.

A similar pattern is observed with respect to the NDMI, with the highest values detected under normal environmental conditions, while they drop under heat wave con-

ditions (Figure 6). In this way, and under the first condition, the highest value is in the vegetation cover (0.372) and the lowest value in the urban land cover (0.113), while the farmland cover has an average value of 0.259. Under heat wave conditions, there is a decrease of 16.13%, 4.42%, and 62.55% in vegetation, urban land, and farmland covers, respectively (Figure 6a). For each of the green areas analysed and under normal environmental conditions, the average value is 0.318, ranging from the highest in Battersea Park (0.398) and Green Park (0.351) to the lowest (0.258) in Clapham Park (Figure 6b). The values suffer a generalized decrease under heat wave conditions, so that the average value is 0.277. This represents an average decrease of 12.89%. The biggest declines are reported in Battersea Park (−20.85%), Burgess Park (−17.07%), and Regent's Park (−12.75%).

3.3. LST

The spatiotemporal evolution of LST under normal ambient conditions and heat wave conditions can be analysed in Figures S7 and S8 of the Supplementary Materials. The average LST under normal conditions is 28.58 °C, while under heat wave conditions, it is 29.98 °C. These values represent an average increase of 1.40 °C (4.66%).

Figure 7a shows how in the different LULC categories of the city, the LST presents lower values under normal conditions than in heat wave conditions. Thus, under normal conditions, the highest average value (29.85 °C) is in the urban land cover, while the lowest value (25.34 °C) is in the vegetation cover. The farmland cover has an average value of 26.92 °C. A similar pattern is observed under heat wave conditions, but with a generalized increase of 5.27%, 2.25%, and 1.72% in the vegetation, urban land, and farmland covers, respectively. Concerning each of the green areas analyzed and under normal environmental conditions, the average value is 26.58 °C, ranging from the highest LST (28.72 °C) for Clapham Park and Burgess Park (28.38 °C) to the lowest (24.89 °C) for Green Park (Figure 7b). This circumstance is related to the fact that these forests have fewer trees than the rest. Tree vegetation not only cools the environment through evapotranspiration but also prevents sunlight from heating the ground surface by casting shadows. The values experience a generalized rise under heat wave conditions, so that the average value is 28.01 °C, which represents an average decrease of 5.46%. The largest declines were reported in Green Park (7.51%) and Regent's Park (6.70%). Therefore, the results show that areas with greater tree cover and aquatic areas have a lower average LST both under normal conditions and during the heat wave. Therefore, the results show that areas with larger aquatic areas (Table 1) and larger tree vegetation (Figure S7) have a lower average LST both under normal conditions and during the heat wave.

In Figures S9 and S10 of the Supplementary Materials, the isolines of LST can be seen both under normal conditions and under heat wave conditions. In both environmental conditions, it is reported that the least warm areas are lakes or aquatic areas, followed by wooded areas. In contrast, the warmest areas are green areas without trees and with grass cover and areas that have small constructions or buildings associated with green areas.

3.4. MTHI

The spatiotemporal analysis of the thermal comfort index (MTHI) of the areas under study and under both environmental conditions can be found in Figures 8 and 9. The average MTHI value of the entire city under normal conditions is 3.03 (hot), while under heat wave conditions, it is 3.17 (hot). These values imply an average increase of 0.14 (4.42%). It can be seen how the areas with the lowest MTHI and, therefore, with better environmental comfort coincide with the areas with the lowest LST, that is, green areas with trees and aquatic areas or lakes. On the other hand, the areas with the highest MTHI and, therefore,

with the lowest environmental comfort are the areas with the highest LST and turf cover and those that have small constructions or buildings.

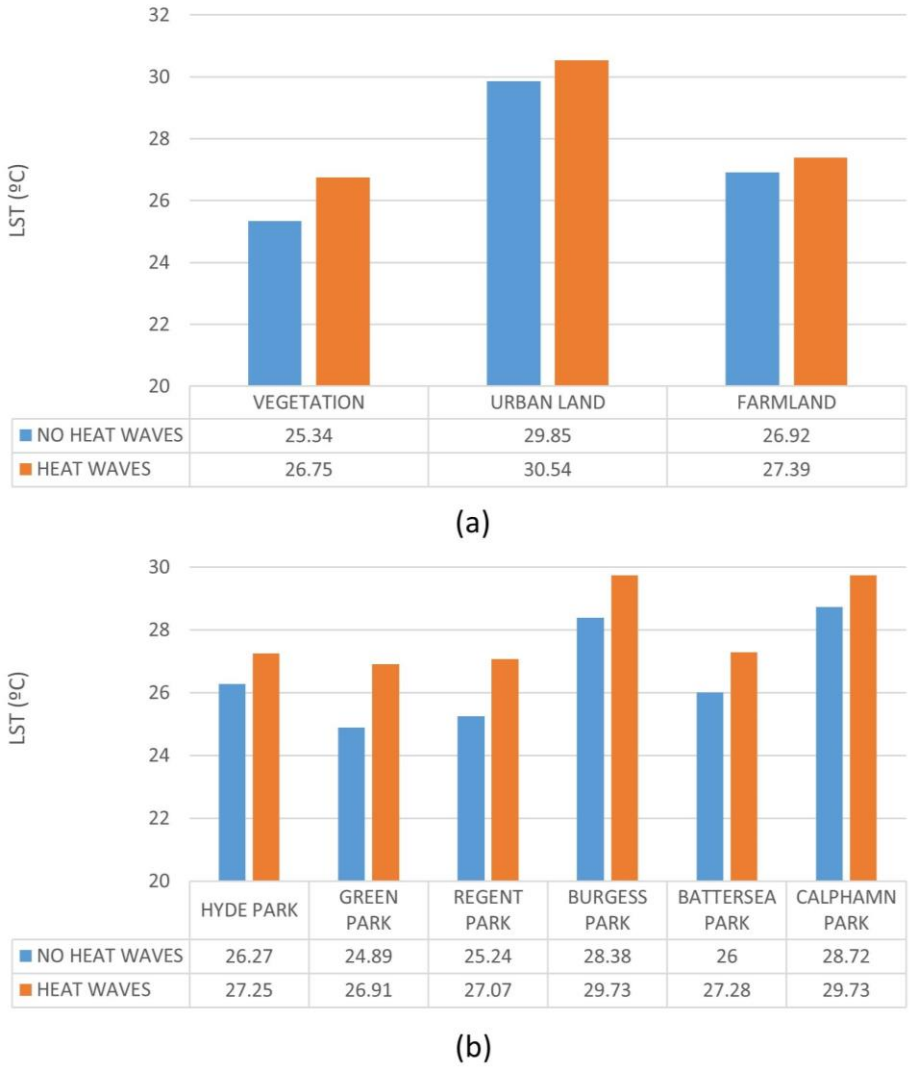

Figure 7. LST under heat wave and non-heat wave (normal) conditions for different LULC classes of the city (**a**) and for different green areas (**b**).

Figure 10a shows how in the different LULC classes of the city, the MTHI presents lower values under normal than under heat wave conditions. Thus, under normal conditions, the highest average value (3.17) is in the urban land cover, while the lowest value (2.63) is in the vegetation cover. The farmland coverage has an average value of 2.79. Under heat wave conditions, the highest and lowest values of the MTHI correspond to the same LULC classes, but with a generalized increase of 8.68%, 4.23%, and 6.38% in vegetation, urban land, and farmland covers, respectively. The average value for each of the green areas studied under normal environmental conditions is 2.50 (slightly hot), ranging from the highest MTHI (2.87) for Clapham Park and Hyde Park (2.59) to the lowest (2.17) for Green Park and 2.27 for Regent's Park (Figure 10b). The values experience a generalized rise under heat wave conditions in such a way that the average value is 3.34 (hot), which represents an average increase of 25.15%. The largest increases were reported in Regent's Park (41.79%) and Burgess Park (33.15%). On the other hand, the smallest increases occurred in Hyde Park (7.82%) and Clapham Park (15.83%). These results reflect several important factors to consider: During extreme heat waves with temperatures above 40 °C, natural vegetation mechanisms become saturated, and therefore, the vegetation mass does not cool as quickly

as under normal conditions, as it cannot compensate for the excess heat. Green areas with less vegetation are also more ventilated and can therefore disperse heat more easily. It is also important to consider the urban areas adjacent to green areas, as these influence the increase in environmental discomfort. That is, green areas located in hot urban areas present worse comfort conditions than green areas located in less warm urban areas. Thus, nearby urban development affects the comfort conditions of green areas when significant temperature increases occur.

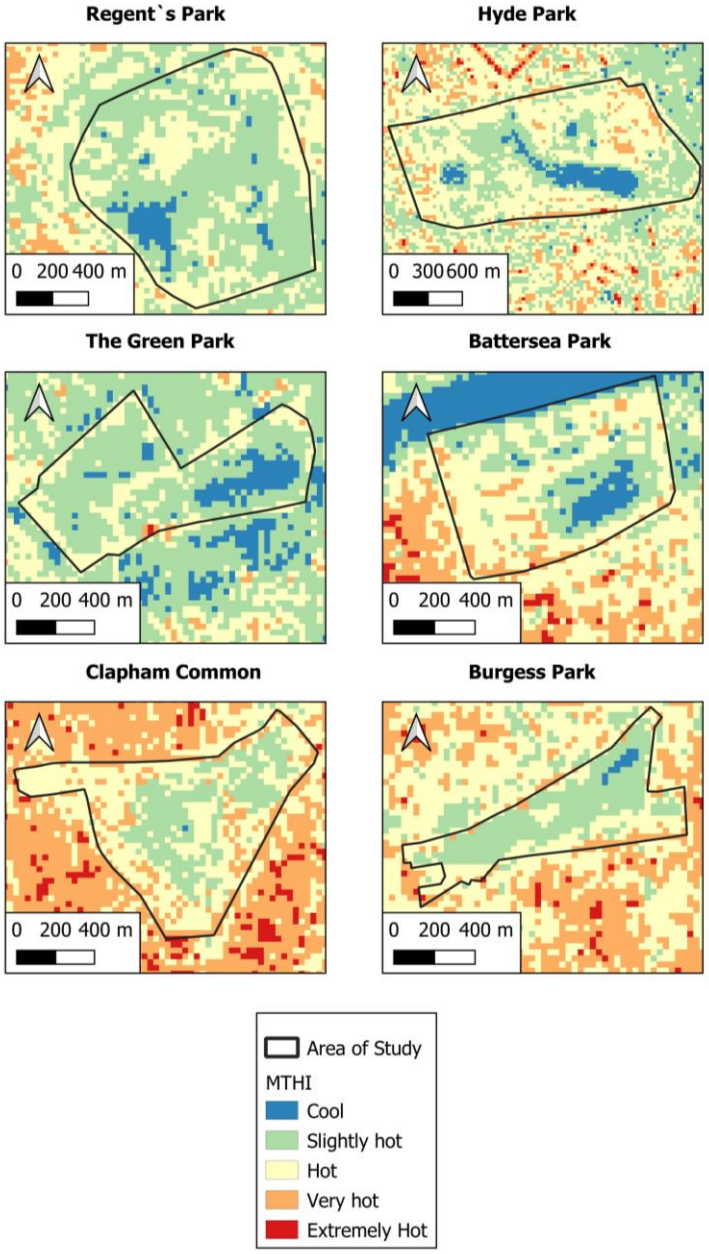

Figure 8. Spatial pattern of MTHI in green areas in the city of London, under normal environmental conditions.

Figure 11 shows how the surface area of each MTHI level in each green zone varies when environmental conditions change from normal to heat wave conditions. In general terms, it is reported that the low MTHI levels (1 and 2), and therefore more comfortable levels, decrease their surface area when there is an increase in temperatures. Conversely, the high MTHI levels (3, 4 and 5), and therefore less comfortable levels, increase their surface area. Noteworthy are the significant increases in the surface areas of level 3 in Green

Park and Regent's Park of 42.22% and 38.28%, respectively, and of level 4 of 18.06% and 19.79%, respectively.

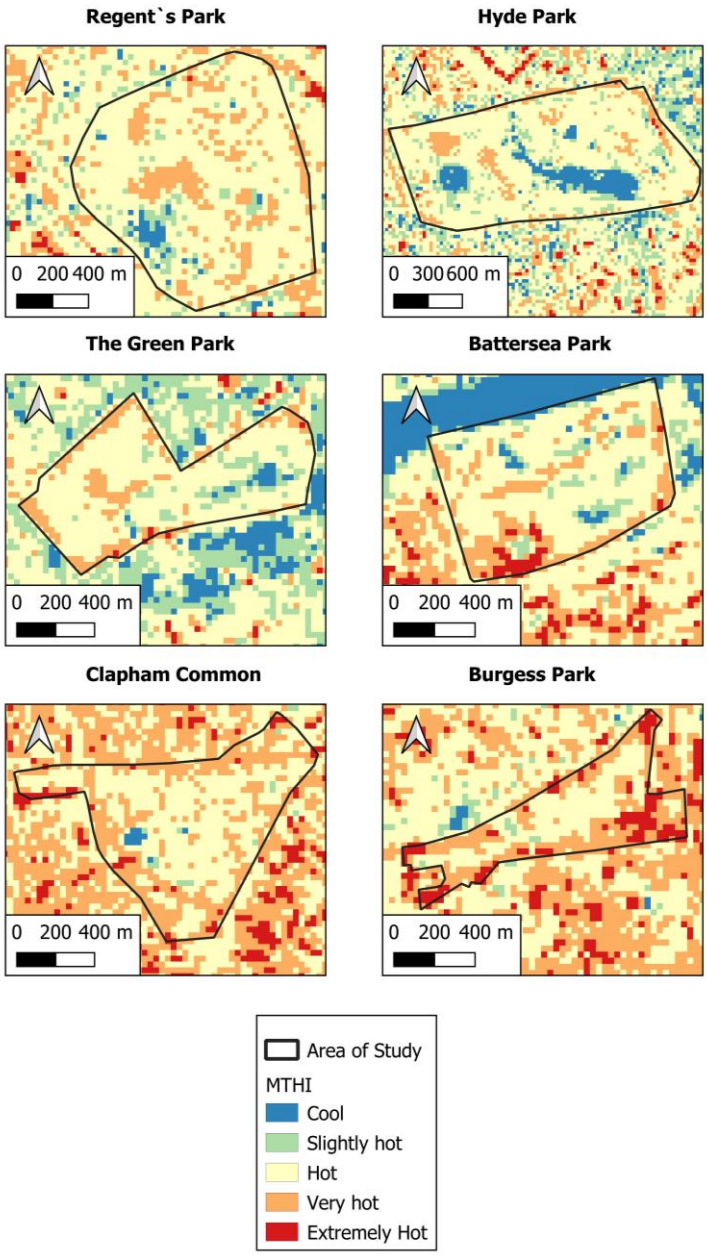

Figure 9. As in Figure 8, but for heat wave environmental conditions.

3.5. Statistical Analysis

3.5.1. ANOVA of Variables

The ANOVA (Table S1 of the Supplementary Materials) applied to the investigated variables (NDVI, NDMI, LST, and MTHI) revealed, through the Shapiro–Wilk test, that the distributions do not follow a normal distribution in the green areas analyzed since the *p*-value was less than 0.05. Due to this, to continue with the ANOVA analysis in cases of non-normal distributions, it was necessary to apply the Kruskal–Wallis test. The results (Table S1) show that all variables analyzed had a *p*-value of 0.000 in each green area analyzed. This circumstance indicates that the variables NDVI, NDMI, LST, and MTHI present statistically significant relationships, with a confidence level greater than 99%, between the different green areas studied. According to the results obtained, it was found

that the variables NDVI, NDMI, LST, and MTHI have statistically significant relationships, with a confidence level higher than 99%, between the different green areas studied. In this way, it is reported that each green area presents specific conditions (location, surface, construction, vegetation, etc.) that influence the variables analyzed and, therefore, modify said variables by presenting differences.

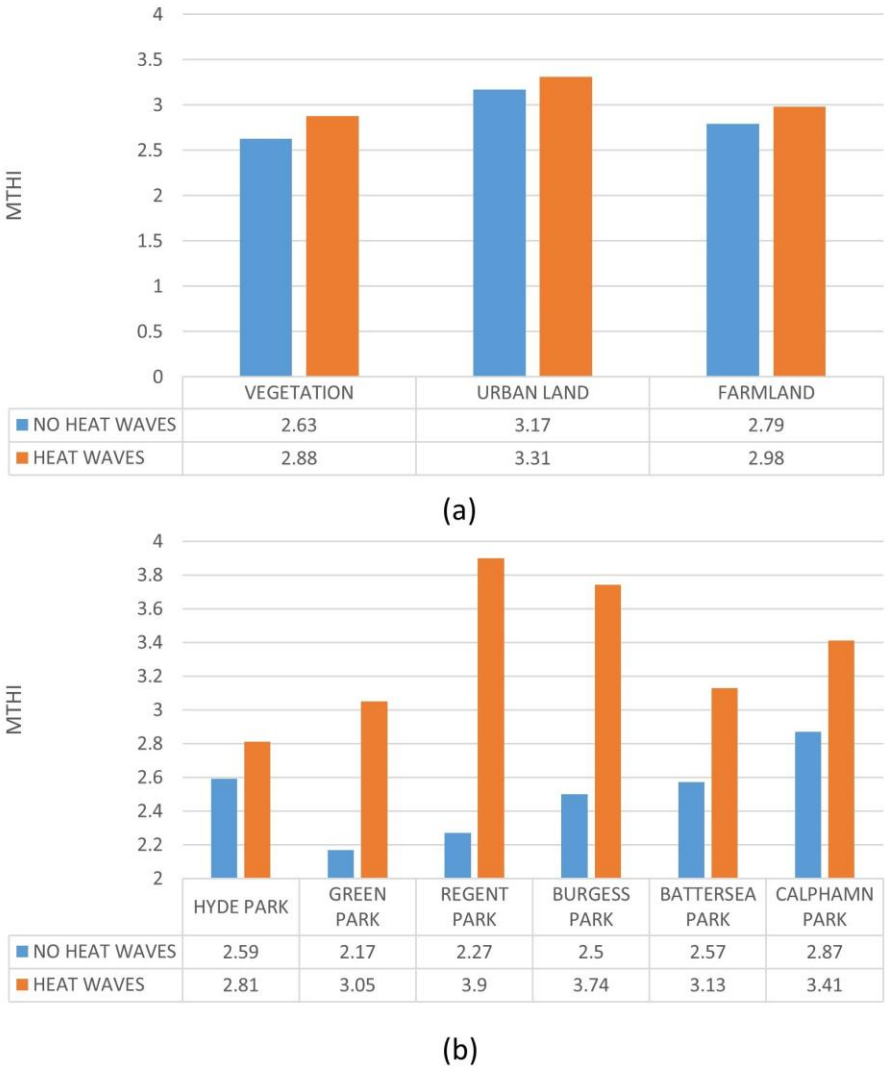

Figure 10. MTHI under heat wave and non-heat wave (normal) conditions for different LULC classes of the city (**a**) and for different green areas (**b**).

3.5.2. Data Panel

First, and since these are parametric data that comply with normal distributions, homogeneity of variances, and independence, the Pearson correlation was determined to obtain the relationship between the variables (Table S2 of the Supplementary Materials). The results show that the MTHI has a strong positive correlation with the LST and NDMI variables and a weak negative correlation with the NDVI variable. All correlations are statistically significant, which leads us to reject the null hypothesis and confirm the correlations between the variables.

Subsequently, the Panel Data and the Generalized Least Squares method were used, the results of which can be consulted in Table 5.

The results of the statistical analysis revealed a significant positive relationship ($p < 0.001$) greater than 99% between the variables MTHI, NDMI, and LST, and a sig-

nificant negative relationship ($p < 0.001$) greater than 99% between MTHI and NDVI. In addition, the values of R^2, F, and Prob > Chi^2 reflect a strong agreement between the variables, greater than 99%.

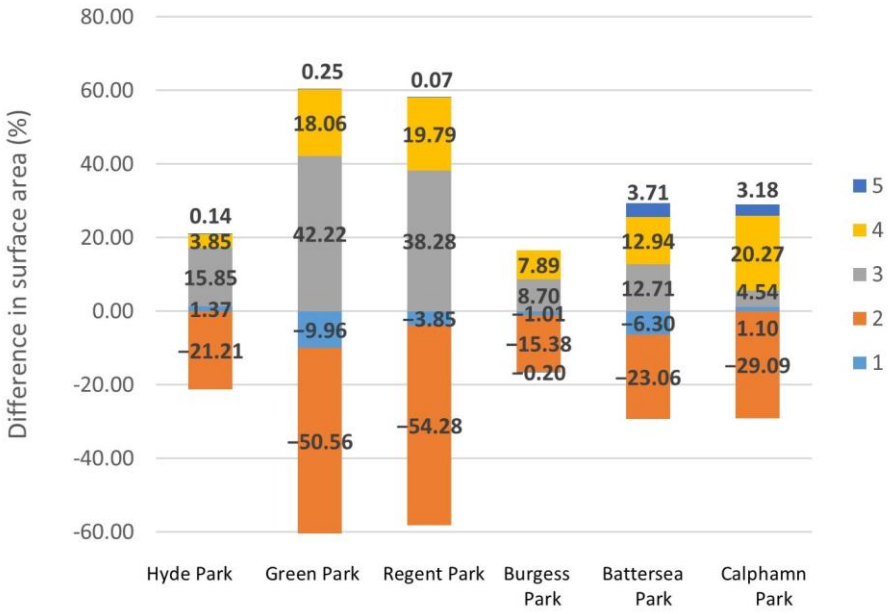

Figure 11. Differences in surface area (%) MTHI between heat wave and non-heat wave conditions, for each comfort level in the six green areas.

Table 5. Results data panel.

Variables	Beta	*p*-Value	Sd
NDVI	−0.3988	0.000	0.0572
NDMI	5.2391	0.000	0.1085
LST	0.3535	0.000	0.0328
	$R^2 = 0.81$	F = 4179.82	Prob > $chi^2 = 0.000$

Note: β: coefficient; R^2: linear regression coefficient; F: statistician F: Sd: standard deviation.

4. Discussion

This research has addressed how heat waves can modify the environmental comfort conditions of the green areas of the city of London. The results obtained are of paramount significance, given the multitude of studies that caution about a surge in heat waves in the forthcoming decades due to climate change [2–4,9,53].

The results suggest that green areas have a cooling effect on the LST of the city, both under normal conditions and during heat waves, and should, therefore, be considered essential infrastructure for temperature mitigation. Our findings are consistent with those of prior research, which show that urbanized and impermeable areas cause an increase in the LST, while the increase in green areas produces a reduction in it [21,49].

During July 2022, the city of London suffered a heat wave that increased ambient temperatures to 40 °C, breaking all temperature records in the country. While such temperatures are unprecedented in UK climate history, according to climate models, temperatures above 40 °C could occur every 3–4 years by the end of the century in the country, under a very high emissions scenario [54–56]. In addition to other atmospheric processes leading to the incidence of this extreme event, dry conditions and a lack of moisture contributed to elevated temperatures, pointing to the important role of green areas and soil moisture feedback [31].

The MTHI thermal index has made it possible to evaluate the thermal comfort of the six green areas investigated and how it has intensified during the heat wave. Thus, during a day of normal environmental conditions, the average MTHI of the green areas was 2.50 (slightly hot), while in heat wave conditions, it rose to an average value of 3.34 (hot). These values imply an average increase of 25.15% and a significant reduction in people's environmental comfort conditions. This variation in the MTHI is consistent with previous studies that highlight the importance of green infrastructure to mitigate urban heat [32]. This evolution of the MTHI demonstrates that even spaces traditionally considered thermal refuge zones can become uncomfortable or even unhealthy under extreme conditions. By linking the MTHI with variables such as the LST, NDMI, and NDVI, it has been possible to identify that the presence of tree vegetation and water bodies effectively contributes to reducing surface temperatures and improving comfort. Thus, the MTHI is positioned as a useful tool not only for assessing the impact of heat waves in real time but also for guiding urban design toward mitigation, adaptation, and thermal resilience strategies. Therefore, the application of the MTHI allows for a spatial and temporal understanding of thermal comfort gradients in the city and, thereby, informs more sustainable planning policies focused on citizen well-being in the face of climate change.

The NDVI and NDMI related to vegetation and soil moisture showed higher values under normal conditions than in ambient heat wave conditions. Conversely, LST presented higher values in heat wave conditions as opposed to periods of normal environmental conditions. These conditions are usually common during periods of heat waves. These results provide scientific evidence of how heat affects the thermal comfort of green areas and are in line with other studies that have used this index to assess thermal comfort in urban areas, for example, in the city of Shanghai (China) in 2024 [32] or Jiangsu (China) [33], that allow us to validate our results.

A key finding of the research is that within green areas, it has been detected that the highest values of LST and MTHI are in areas that have buildings or soil with grass cover. On the other hand, the lowest LST values and better comfort conditions are in green areas with trees or areas with water or lakes. This circumstance has already been analyzed and studied in other studies [22,29,30,57–60], obtaining similar results and validating those obtained in this research. This circumstance is motivated by the shadows produced by the trees, which reduce the solar radiation received and increase evapotranspiration. Both issues reduce the LST of this wooded area.

Another option corroborated here and of great importance is the use of Blue Infrastructure (BI) such as lakes and ponds as an element to minimize LST and improve thermal comfort. Thus, those green areas with smaller surfaces of lakes and ponds (Table 1) present worse environmental comfort conditions and LST. Some studies have reported that these can reduce temperatures by 11.33% for every 10% increase in coverage [60]. On the other hand, lawn areas or areas with associated buildings receive solar radiation and heat up by subsequently dumping that heat into the atmosphere. This situation has been investigated by other authors [6,61], who have reached conclusions like those presented in this study.

The results of this study have significant implications for the development of environmental policies focused on optimizing green areas as thermal mitigation tools in urban environments. By providing empirical evidence on the thermal resilience of these areas, our findings can contribute to the design of urban planning strategies that minimize the effects of urban warming and improve population thermal comfort. Thus, the construction of wooded green areas and the use of BI reduce temperatures and improve the quality of life of visitors to these areas, as has been corroborated in numerous studies [22,59,60].

Metropolitan forests provide significant advantages for thermal comfort and climate resilience; yet, their establishment and maintenance can pose challenges, particularly in

populated or resource-constrained metropolitan destinations. To address this, native and drought-resistant flora should be prioritized since they can significantly decrease irrigation and maintenance needs. Secondly, community-based and volunteer activities can enhance long-term care while simultaneously enhancing public engagement in the protection of these areas.

Additionally, one of the main contributions of this study lies in the applicability and replicability of the methodology employed [62,63]. The availability of open-access data and the non-intrusive nature of the methodology facilitate its implementation in future studies, favouring the development of sustainability and adaptive urban planning programs [64].

5. Conclusions

In this research, modification of the MTHI Environmental Comfort Index has been studied in six urban forests in the city of London during July 2022. Our findings:

- Underscored the impact of elevated temperatures from heat waves on the thermal comfort of individuals in green spaces. This situation affects individuals and has future implications for these regions due to the anticipated rise in occurrences of extreme temperatures in the years to come.
- Investigated the environmental discomfort measured by the MTHI, which goes from 2.5 (slightly hot) to 3.34 (hot) in heat wave conditions. This indicates a substantial increase that considerably affects the environmental comfort of the people who visit these areas to alleviate the effects of high temperatures in urban areas.
- Reported that the promotion of green areas with trees and the use of BIs increase humidity and reduce temperatures, improving the thermal comfort of people who visit the place.
- Provided a key contribution to the effectiveness of green space temperature mitigation during heat waves in a city unfamiliar with these events.
- Offered a new methodology that allows for the analysis of comfort conditions in a way that can be easily extrapolated to other locations.
- Highlighted the importance of conducting additional studies that explore how climate change and heat waves will impact not only green areas but also the various activities that people carry out in them.
- Revealed the need to implement mitigation and resilience measures in both urban areas and green spaces.
- Suggested the urgent need to implement policies that prioritize climate resilience in green area planning. It is crucial to promote the development of green and blue infrastructure, as well as to increase the density of tree cover to improve thermal comfort and mitigate the effects of heat waves to make them more resilient to climate change. In this way, the integration of thermal comfort in the planning and management of spaces must be considered a fundamental element of public administration. In sum, the following actionable insights for policymakers are suggested:
- Increase tree density in urban green spaces: trees considerably lower temperatures and provide comfort during heat waves.
- Enhance tree coverage by choosing native and drought-resistant varieties.
- Preserve shade and evapotranspiration benefits by the regular maintenance of plants.
- Invest in green and blue infrastructure: such facilities reduce heat stress and promote climate resilience over time.
- Incorporate thermal comfort indices such as MTHI into urban planning to enhance the evaluation and design of public spaces that are appropriate for future climate conditions.

- Prioritize climatic adaptability when constructing ecological zones: cities must plan for increased frequency of heat waves and implement suitable measures.
- Identify sensitive areas and people: use geographical data to determine the areas where interventions such as planting and shade are most needed.
- Advocate for transdisciplinary urban climate research: policies should be based on robust and scalable methodologies and the results of scientific studies.

6. Limitations

This study has several limitations. First, no in situ measurements were made; instead, the analysis relied solely on remotely sensed data sources. This could affect the accuracy of specific environmental indicators. Future research recommends including in situ measurements, such as direct measurements of temperature, relative humidity, or thermal perception by park users, to improve upon results obtained through remote sensing. Integrating surface environmental sensors and user surveys into future studies would allow comparison of satellite indices with actual thermal experience, improving the robustness and applicability of the conclusions. Another limitation is that this study did not determine species-specific variations in trees, which could influence the effectiveness of thermal regulation. This may provide an avenue for future studies to examine the role of this factor in thermal comfort.

Supplementary Materials: The following supporting information can be downloaded at: https://www.mdpi.com/article/10.3390/f16050790/s1. Figure S1. 3D image of the green areas investigated. Source: Prepared by the authors using Google Earth images. Figure S2. Relationships between LST, NDMI and MTHI. Figure S3. Spatial pattern of NDVI in green areas in the city of London, under normal ambient conditions. Figure S4. As in Figure S3 but for heat wave environmental conditions. Figure S5. Spatial pattern of NDMI at green areas in the city of London, under normal ambient conditions. Figure S6. As in Figure S5 but for heat wave environmental conditions. Figure S7. Spatial pattern of LST in green areas in the city of London, under normal environmental conditions. Figure S8. As in Figure S7 but for heat wave environmental conditions. Figure S9. LST isolines at green areas in the city of London, under normal environmental conditions. Figure S10. As in Figure S9 but for heat wave environmental conditions. Table S1. ANOVA test results for variables NDVI, NDMI, LST Y MTHI. Table S2. Pearson correlation coefficient and *p* value between MTHI and other variables investigated.

Author Contributions: Conceptualization, D.H.-G., D.F., H.R., A.E.J. and M.A.; methodology, D.H.-G., D.F., H.R., A.E.J. and M.A.; software, D.H.-G., D.F., H.R., A.E.J. and M.A.; validation, D.H.-G., D.F., H.R., A.E.J. and M.A.; formal analysis, D.H.-G., D.F., H.R., A.E.J. and M.A.; investigation, D.H.-G., D.F., H.R., A.E.J. and M.A.; resources, D.H.-G., D.F., H.R., A.E.J. and M.A.; data curation, D.H.-G., D.F., H.R., A.E.J. and M.A.; writing—original draft preparation, D.H.-G., D.F., H.R., A.E.J. and M.A.; writing—review and editing, D.H.-G., D.F., H.R., A.E.J. and M.A.; visualization, D.H.-G., D.F., H.R., A.E.J. and M.A.; supervision, D.H.-G., D.F., H.R., A.E.J. and M.A.; project administration, D.H.-G., D.F., H.R., A.E.J. and M.A. All authors have read and agreed to the published version of the manuscript.

Funding: This research received no external funding.

Data Availability Statement: Data will be available upon request to the corresponding author.

Conflicts of Interest: The authors declare no conflicts of interest.

References

1. Song, J.; Chen, W.; Zhang, J.; Huang, K.; Hou, B.; Prishchepov, A.V. Effects of building density on land surface temperature in China: Spatial patterns and determinants. *Landsc. Urban Plan.* **2020**, *198*, 103794. [CrossRef]
2. MCGregor, G.R.; Felling, M.; Wolf, T.; Gosling, S. *The Social Impacts of Heat Waves*; Environment Agency: Bristol, UK, 2007; 41p.

3. Lemonsu, A.; Viguié, V.; Daniel, M.; Masson, V. Vulnerability to heat waves: Impact of urban expansion scenarios on urban heat island and heat stress in Paris (France). *Urban Clim.* **2015**, *14*, 586–605. [CrossRef]
4. Li, D.; Bou-Zeid, E. Synergistic interactions between urban heat islands and heat waves: The impact in cities is larger than the sum of its parts. *J. Appl. Meteorol. Climatol.* **2013**, *52*, 2051–2064. [CrossRef]
5. Li, J.; Song, C.; Cao, L.; Zhu, F.; Meng, X.; Wu, J. Impacts of landscape structure on surface urban heat islands: A case study of Shanghai, China. *Remote Sens. Environ.* **2011**, *115*, 3249–3263. [CrossRef]
6. Hidalgo García, D.; Arco Díaz, J. Modeling of the Urban Heat Island on local climatic zones of a city using Sentinel 3 images: Urban determining factors. *Urban Clim.* **2021**, *37*, 100840. [CrossRef]
7. Stewart, I.D.; Oke, T.R. Local climate zones for urban temperature studies. *Bull. Am. Meteorol. Soc.* **2012**, *93*, 1879–1900. [CrossRef]
8. Arnfield, A.J. Two decades of urban climate research: A review of turbulence, exchanges of energy and water, and the urban heat island. *Int. J. Climatol.* **2003**, *23*, 1–26. [CrossRef]
9. Hidalgo, D. Analysis of synergies between the Urban Heat Island and Heat Waves using Sentinel 3 satellite images: Study of Andalusian cities (Spain). *Earth Syst. Environ.* **2021**, *6*, 199–219. [CrossRef]
10. ONU. Una Población en Crecimiento. 2020. Available online: https://www.un.org/es/global-issues/population (accessed on 7 May 2025).
11. Mukherjee, F.; Singh, D. Assessing Land Use–Land Cover Change and Its Impact on Land Surface Temperature Using LANDSAT Data: A Comparison of Two Urban Areas in India. *Earth Syst. Environ.* **2020**, *4*, 385–407. [CrossRef]
12. Guo, A.; Yang, J.; Xiao, X.; Xia, J.; Jin, C.; Li, X. Influences of urban spatial form on urban heat island effects at the community level in China. *Sustain. Cities Soc.* **2020**, *53*, 101972. [CrossRef]
13. Hidalgo García, D.; Rezapouraghdam, H. Climate change, heat stress and the analysis of its space-time variability in european metropolises. *J. Clean. Prod.* **2023**, *425*, 138892. [CrossRef]
14. Karakuş, C.B. The Impact of Land Use/Land Cover (LULC) Changes on Land Surface Temperature in Sivas City Center and Its Surroundings and Assessment of Urban Heat Island. *Asia Pac. J. Atmos. Sci.* **2019**, *55*, 669–684. [CrossRef]
15. Santamouris, M. Recent progress on urban overheating and heat island research. Integrated assessment of the energy, environmental, vulnerability and health impact. Synergies with the global climate change. *Energy Build.* **2020**, *207*, 109482. [CrossRef]
16. Mora, C.; Dousset, B.; Caldwell, I.R.; Powell, F.E.; Geronimo, R.C.; Bielecki, C.R.; Counsell, C.W.; Dietrich, B.S.; Johnston, E.T.; Louis, L.V.; et al. Global risk of deadly heat. *Nat. Clim. Change* **2017**, *7*, 501–506. [CrossRef]
17. Meehl, G.A.; Tebaldi, C. More intense, more frequent, and longer lasting heat waves in the 21st century. *Science* **2004**, *305*, 994–997. [CrossRef]
18. Sun, Y.; Zhang, X.; Zwiers, F.W.; Song, L.; Wan, H.; Hu, T.; Yin, H.; Ren, G. Rapid increase in the risk of extreme summer heat in Eastern China. *Nat. Clim. Change* **2014**, *4*, 1082–1085. [CrossRef]
19. An, N.; Dou, J.; González-Cruz, J.E.; Bornstein, R.D.; Miao, S.; Li, L. An observational case study of synergies between an intense heat wave and the urban heat island in Beijing. *J. Appl. Meteorol. Climatol.* **2020**, *59*, 605–620. [CrossRef]
20. Coumou, D.; Robinson, A.; Rahmstorf, S. Global increase in record-breaking monthly-mean temperatures. *Clim. Change* **2013**, *118*, 771–782. [CrossRef]
21. Saaroni, H.; Amorim, J.H.; Hiemstra, J.A.; Pearlmutter, D. Urban Green Infrastructure as a tool for urban heat mitigation: Survey of research methodologies and findings across different climatic regions. *Urban Clim.* **2018**, *24*, 94–110. [CrossRef]
22. Hidalgo García, D. Spatio-temporal analysis of the urban green infrastructure of the city of Granada (Spain) as a heat mitigation measure using high-resolution images Sentinel 3. *Urban For. Urban Green.* **2023**, *87*, 128061. [CrossRef]
23. Gago, E.J.; Roldan, J.; Pacheco-Torres, R.; Ordóñez, J. The city and urban heat islands: A review of strategies to mitigate adverse effects. *Renew. Sustain. Energy Rev.* **2013**, *25*, 749–758. [CrossRef]
24. Solecki, W.D.; Rosenzweig, C.; Parshall, L.; Pope, G.; Clark, M.; Cox, J.; Wiencke, M. Mitigation of the heat island effect in urban New Jersey. *Environ. Hazards* **2005**, *6*, 39–49. [CrossRef]
25. Oliveira, A.; Lopes, A.; Niza, S. Local climate zones in five southern European cities: An improved GIS-based classification method based on Copernicus data. *Urban Clim.* **2020**, *33*, 100631. [CrossRef]
26. Dwivedi, A.; Mohan, B.K. Impact of green roof on micro climate to reduce Urban Heat Island. *Remote Sens. Appl.* **2018**, *10*, 56–69. [CrossRef]
27. Masoudi, M.; Tan, P.Y.; Fadaei, M. The effects of land use on spatial pattern of urban green spaces and their cooling ability. *Urban Clim.* **2021**, *35*, 100743. [CrossRef]
28. Qiu, G.Y.; Zou, Z.; Li, X.; Li, H.; Guo, Q.; Yan, C.; Tan, S. Experimental studies on the effects of green space and evapotranspiration on urban heat island in a subtropical megacity in China. *Habitat. Int.* **2017**, *68*, 30–42. [CrossRef]
29. Yoshida, A.; Hisabayashi, T.; Kashihara, K.; Kinoshita, S.; Hashida, S. Evaluation of effect of tree canopy on thermal environment, thermal sensation, and mental state. *Urban. Clim.* **2015**, *14*, 240–250. [CrossRef]

30. Spronken-Smith, R.A.; Oke, T.R. The thermal regime of urban parks in two cities with different summer climates. *Int. J. Remote Sens.* **1998**, *19*, 2085–2104. [CrossRef]
31. Met Office. Summer 2022: A Historic Season for Northern Hemisphere Heat Waves. 2022. Available online: https://www.metoffice.gov.uk/blog/2022/summer-2022-a-historic-season-for-northern-hemisphere-heatwaves (accessed on 7 May 2025).
32. Yang, L.; Yang, C.; Zhou, W.; Chen, X.; Wang, C.; Liu, L. Mapping the Spatial and Seasonal Details of Heat Health Risks in Different Local Climate Zones: A Case Study of Shanghai, China. *Remote Sens.* **2024**, *16*, 3513. [CrossRef]
33. Feng, L.; Zhao, M.; Zhou, Y.; Zhu, L.; Tian, H. The seasonal and annual impacts of landscape patterns on the urban thermal comfort using Landsat. *Ecol. Indic.* **2020**, *110*, 105798. [CrossRef]
34. Met Office. Unprecedented Extreme Heat Wave, July 2022. 2022. Available online: https://www.metoffice.gov.uk/binaries/content/assets/metofficegovuk/pdf/weather/learn-about/uk-past-events/interesting/2022/2022_03_july_heatwave_v1.pdf (accessed on 7 May 2025).
35. Howarth, C.; Mcloughlin, N.; Armstrong, A.; Murtagh, E.; Mehryar, S.; Beswick, A.; Ward, B.; Ravishankar, S.; Stuart-Watt, A. *Turning up the Heat Learning from the Summer 2022 Heat Waves in England to Inform UK Policy on Extreme Heat Evidence Report*; Grantham Research Institute on Climate Change and the Environment, London School of Economics and Political Science: London, UK, 2024. Available online: www.lse.ac.uk/granthaminstitute (accessed on 7 May 2025).
36. Hidalgo-García, D.; Arco-Díaz, J. Modeling the Surface Urban Heat Island (SUHI) to study of its relationship with variations in the thermal field and with the indices of land use in the metropolitan area of Granada (Spain). *Sustain. Cities Soc.* **2022**, *87*, 104166. [CrossRef]
37. Yoo, C.; Han, D.; Im, J.; Bechtel, B. Comparison between convolutional neural networks and random forest for local climate zone classification in mega urban areas using Landsat images. *ISPRS J. Photogramm. Remote Sens.* **2019**, *157*, 155–170. [CrossRef]
38. Chavez, P.S. An improved dark-object subtraction technique for atmospheric scattering correction of multispectral data. *Remote Sens. Environ.* **1988**, *24*, 459–479. [CrossRef]
39. García, D.H.; Díaz, J.A. Spatial and multi-temporal analysis of land surface temperature through landsat 8 images: Comparison of algorithms in a highly polluted city (Granada). *Remote Sens.* **2021**, *13*, 1012. [CrossRef]
40. Congedo, L. Semi-Automatic Classification Plugin Documentation Release 4.8.0.1. *Release* **2016**, *4*, 29. Available online: https://media.readthedocs.org/pdf/semiautomaticclassificationmanual-v4/latest/semiautomaticclassificationmanual-v4.pdf (accessed on 7 May 2025).
41. García, D.H.; Díaz, J.A. Space–time analysis of the earth's surface temperature, surface urban heat island and urban hotspot: Relationships with variation of the thermal field in Andalusia (Spain). *Urban Ecosyst.* **2023**, *26*, 525–546. [CrossRef]
42. Yu, X.; Guo, X.; Wu, Z. Land surface temperature retrieval from landsat 8 TIRS-comparison between radiative transfer equation-based method, split window algorithm and single channel method. *Remote Sens.* **2014**, *6*, 9829–9852. [CrossRef]
43. Kafer, P.S.; Rolim, S.B.A.; Iglesias, M.L.; Da Rocha, N.S.; Diaz, L.R. Land surface temperature retrieval by landsat 8 thermal band: Applications of laboratory and field measurements. *IEEE J. Sel. Top. Appl. Earth Obs. Remote Sens.* **2019**, *12*, 2332–2341. [CrossRef]
44. Weng, Q.; Lu, D.; Schubring, J. Estimation of land surface temperature-vegetation abundance relationship for urban heat island studies. *Remote Sens. Environ.* **2004**, *89*, 467–483. [CrossRef]
45. Sharma, R.; Pradhan, L.; Kumari, M.; Bhattacharya, P. Assessing urban heat islands and thermal comfort in Noida City using geospatial technology. *Urban. Clim.* **2021**, *35*, 100751. [CrossRef]
46. Shafri, H.Z.M.; Ramle, F.S.H. A Comparison of Support Vector Machine and Decision Tree Classifications Using Satellite Data of Langkawi Island. *Inf. Technol. J.* **2009**, *8*, 64–70. [CrossRef]
47. Otukei, J.R.; Blaschke, T. Land cover change assessment using decision trees, support vector machines and maximum likelihood classification algorithms. *Int. J. Appl. Earth Obs. Geoinf.* **2010**, *12*, S27–S31. [CrossRef]
48. Amindin, A.; Pouyan, S.; Pourghasemi, H.R.; Yousefi, S.; Tiefenbacher, J.P. Spatial and temporal analysis of urban heat island using Landsat satellite images. *Environ. Sci. Pollut. Res.* **2021**, *28*, 41439–41450. [CrossRef]
49. Wu, P.; Yin, Z.; Yang, H.; Wu, Y.; Ma, X. Reconstructing geostationary satellite land surface temperature imagery based on a multiscale feature connected convolutional neural network. *Remote Sens.* **2019**, *11*, 300. [CrossRef]
50. Alcock, I.; White, M.P.; Lovell, R.; Higgins, S.L.; Osborne, N.J.; Husk, K.; Wheeler, B.W. What accounts for "England's green and pleasant land"? A panel data analysis of mental health and land cover types in rural England. *Landsc. Urban Plan.* **2015**, *142*, 38–46. [CrossRef]
51. Meng, X.; Cheng, J.; Zhao, S.; Liu, S.; Yao, Y. Estimating land surface temperature from Landsat-8 data using the NOAA JPSS enterprise algorithm. *Remote Sens.* **2019**, *11*, 155. [CrossRef]
52. Fang, L.; Tian, C. Construction land quotas as a tool for managing urban expansion. *Landsc. Urban Plan.* **2020**, *195*, 103727. [CrossRef]
53. Sarrat, C.; Lemonsu, A.; Masson, V.; Guedalia, D. Impact of urban heat island on regional atmospheric pollution. *Atmos. Environ.* **2006**, *40*, 1743–1758. [CrossRef]

54. Du, J.; Xiang, X.; Zhao, B.; Zhou, H. Impact of urban expansion on land surface temperature in Fuzhou, China using Landsat imagery. *Sustain. Cities Soc.* **2020**, *61*, 102346. [CrossRef]
55. Feizizadeh, B.; Blaschke, T. Examining Urban heat Island relations to land use and air pollution: Multiple endmember spectral mixture analysis for thermal remote sensing. *IEEE J. Sel. Top. Appl. Earth Obs. Remote Sens.* **2013**, *6*, 1749–1756. [CrossRef]
56. Christidis, N.; McCarthy, M.; Stott, P.A. The increasing likelihood of temperatures above 30 to 40 °C in the United Kingdom. *Nat. Commun.* **2020**, *11*, 3093. [CrossRef] [PubMed]
57. Hidalgo García, D.; Arco Díaz, J.; Martín Martín, A.; Gómez Cobos, E. Spatiotemporal Analysis of Urban Thermal Effects Caused by Heat Waves through Remote Sensing. *Sustainability* **2022**, *14*, 12262. [CrossRef]
58. Brown, R.D.; Vanos, J.; Kenny, N.; Lenzholzer, S. Designing urban parks that ameliorate the effects of climate change. *Landsc. Urban Plan.* **2015**, *138*, 118–131. [CrossRef]
59. Cheng, Y.; Bartesaghi-Koc, C.; Tian, Y.; Shen, L.; Teng, M.; Liu, H.; Xiao, Z.; Zhang, B.; Wu, C. Where and how to cool through blue infrastructure? Large lake groups to ameliorate urban overheating in a typical inland multi-lake megacity. *Sustain. Cities Soc.* **2023**, *98*, 104869. [CrossRef]
60. Lin, Y.; Wang, Z.; Jim, C.Y.; Li, J.; Deng, J.; Liu, J. Water as an urban heat sink: Blue infrastructure alleviates urban heat island effect in mega-city agglomeration. *J. Clean. Prod.* **2020**, *262*, 121411. [CrossRef]
61. Chun, B.; Guldmann, J.M. Spatial statistical analysis and simulation of the urban heat island in high-density central cities. *Landsc. Urban Plan.* **2014**, *125*, 76–88. [CrossRef]
62. Puga-Bonilla, M.; Hidalgo-García, D.; Rezapouraghdam, H.; Bolivar, F.J.L. Risk of mortality and disease attributable to the heat stress index and its variability during heat waves: An observational study on the city of Madrid. *Sustain. Cities Soc.* **2025**, *121*, 106189. [CrossRef]
63. Hidalgo-García, D.; Founda, D.; Rezapouraghdam, H. Spatiotemporal variability of the Universal Thermal Climate Index during heat waves using the UrbClim climate model: Implications for tourism destinations. *Urban Clim.* **2025**, *59*, 102281. [CrossRef]
64. Rezapouraghdam, H.; Hidalgo-García, D. Urban Development and Climate Change: Implications for Educational Tourism Destination Planning. *Water Air Soil. Pollut.* **2024**, *235*, 319. [CrossRef]